www.ietdl.org

Published in IET Microwaves, Antennas & Propagation
Received on 23rd April 2011
Revised on 26th July 2011
doi: 10.1049/iet-map.2011.0194

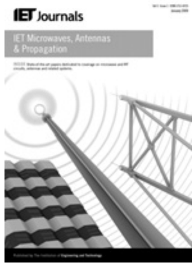

ISSN 1751-8725

In-plane cavity-backed coplanar waveguide to rectangular waveguide transition

M. Vahidpour K. Sarabandi

Radiation Laboratory, Department of Electrical Engineering and Computer Science, University of Michigan, Ann Arbor, Michigan, USA
E-mail: mvahid@umich.edu; saraband@eecs.umich.edu

Abstract: A transition from cavity-backed coplanar waveguide (CBCPW) to rectangular waveguide using a short-circuited pin in conjunction with resonant sections of coplanar waveguide (CPW) and reduced height waveguide segments is presented. The proposed transition is designed with prismatic features in order to ease the fabrication process. An equivalent circuit model is developed to facilitate the design procedure and full-wave analysis is used to optimise the design. As an example a transition operating at Ka-band is designed and shown to have insertion loss of less than 1 dB and reflection below −10 dB over 9% of bandwidth for a back-to-back structure. To further validate the results a prototype transition at Ka-band for a standard WR-28 rectangular waveguide was fabricated and tested. The measured *S*-parameters of the prototype show a very good agreement with the simulation results.

The increasing demand for microwave and millimetre-wave monolithic integrated circuits has led to the development and implementation of coplanar waveguides (CPWs). CPW lines are commonly used at millimetre-wave frequencies because of their compact planar geometry and ease of integration with shunt and series elements which eliminates the need to process backside and the use of via holes. In addition, the design of microwave probes for on-wafer characterisation of millimetre-wave-integrated circuits is another important motivation to employ CPW lines. However, in all planar transmission lines, loss increases by frequency. On the other hand, rectangular waveguides are widely used at higher frequencies as antenna feeds and filters because of their high *Q*-factor, low-loss characteristics and high-power handling capabilities. Owing to these features, it is common to see submillimetre- and millimetre-wave devices combine waveguide components with CPW lines. For such devices, obviously an appropriate low-loss transition is required.

Various microstrip-to-waveguide [1–3] and CPW-to-rectangular waveguide transitions have been proposed in the past. These transitions are either along or perpendicular to the direction of propagation. The cosine tapered ridge [4, 5] and ridge-through waveguide [6] transitions along the propagation direction of the waveguide have been studied at X- and Ka-bands and shown to be broadband while they suffer from their electrically large dimensions. Another set of broadband designs are proposed based on a transition from a rectangular waveguide to antipodal finline [7], which also employ an electrically long substrate in the waveguide. This transition also requires an additional finline to CPW transition. In [8], by employing a tapered slotline probe and a quarter-wavelength impedance transformer, a unified transition is proposed and demonstrated at X-band. This transition could be realised irrespective of the permittivity of the substrate, but has a limited bandwidth for the high-permittivity substrates [9]. To overcome this problem, in [10], a multi-section transformer is employed for wideband matching. Recently, a uniplanar transition based on the tapered finline has been reported with an insertion loss of less than 1 dB with 9% bandwidth at Ka-band [11]. These techniques, however, involve a high degree of fabrication complexity which cannot be easily adopted to silicon or other types of microfabrication techniques.

The transitions transverse to the direction of propagation are mainly based on the extension of a suspended resonant probe from one guiding structure to another. CPW-to-waveguide transitions are similar to coaxial line-to-waveguide transitions [12–14] while the dimensions of the suspended probe and the distance to the backshort have to be carefully designed and optimised. The common feature of all these transitions is suspended probes or other 3D structures inside the waveguide which are not amenable for microfabrication. A transition using uniplanar quasi-Yagi antenna has been reported for wide bandwidth and easy integration at X-band, but suffers from utilising a high-permittivity substrate in order to fit the antenna inside the rectangular waveguide [15]. In the end-launcher aperture-coupled approach [16], the CPW line with the substrate is centred in the waveguide with the centre conductor formed an *L*-shaped loop to couple power to the waveguide mode.

As the frequency increases and the dimensions of the line and waveguide shrink, conventional machining techniques fail to provide the required tolerance. The literature concerning mirofabricating waveguide structures at W-band and higher frequencies is rather sparse. There have been several attempts to fabricate W-band waveguides with low-cost microfabrication techniques such as lithography [17, 18]. However, in these techniques, the height of the waveguide is limited by the maximum thickness of the spun photoresist, limiting the fabrication to the reduced-height waveguides which suffer from high attenuation. Taking advantage of the 'snap-together' technique, a rectangular waveguide was fabricated in two halves and then the halves were put together to form a complete waveguide [19–21]. An alternate technique to etch the waveguide is deep reactive ion etching (DRIE) of silicon. Unlike wet etching which is dependent on the crystal planes of silicon, DRIE is isotropic and provides vertical sidewalls. Hence, DRIE is a viable approach for fabrication of a high-performance micromachined waveguide structure. In [22, 23], a transition using microfabrication processes with separately fabricated and assembled probe has been reported for both diamond and rectangular waveguide with 20% bandwidth. Another high-precision silicon micromachined transition with a capability to integrate filters has been proposed in [24, 25] and shows wideband characteristics at the same frequency range. However, limitations of microfabrication processes do not allow fabricating many of the aforementioned transitions because of the complexity of the geometries and the number of steps needed in their assembly.

In this study, we propose an in-plane cavity-backed coplanar waveguide (CBCPW) line-to-rectangular waveguide transition with prismatic features that does not require multiple parts and complex assembly. In this approach, the need for fabricating suspended probe is eliminated and effective transition is achieved using two resonant structures, namely, shorted CPW line over the waveguide followed by an *E*-plane step discontinuity. Since the design is very simple with the features aligned with the Cartesian coordinate planes, it is highly compatible with microfabrication processes. However, it should be mentioned that since the design is using short-circuited pin, the transition bandwidth is somewhat limited. The transition is modelled by an equivalent circuit to help with the initial design which is then optimised using a full-wave analysis. To demonstrate the validity of the transition and its model, a back-to-back structure is fabricated by conventional machining methods at Ka-band and the measurement results are compared to the simulations.

1 Design considerations of waveguide transitions

Traditional transitions based on *E*-plane probe excitation of the waveguide mode involve attaching a suspended probe to the centre conductor of CPW or coaxial lines perpendicular to the broad wall of waveguides as shown in Fig. 1*a*. The suspended probes in waveguide can be viewed as an infinite array of dipoles and thus can be matched rather easily to a coaxial line and provide octave bandwidth. The coaxial line-to-waveguide transitions are commonly used at microwave frequencies since fabrication and assembly is rather straightforward. At high millimetre-wave and submillimetre-wave frequencies where dimensions are very small, suspending small metalised probes and assembly with the required tolerance is a challenging task. If the probe is extended, all the way to the lower plate of the waveguide to form a shorting pin then the pin can be formed on same substrate and can be bonded to a top substrate to make the required electric connection. However, a short-circuited probe is not resonant, acts purely reactive and cannot be matched to the CPW line directly. In the next section, the architecture needed for making the transition from CPW to rectangular waveguide using a shorting pin is described.

2 Transition using a shorting pin

To properly excite a waveguide with a shorting pin, a resonant condition must be achieved to eliminate the reactance of the pin. It is well known that a pin terminated by the broad wall of a rectangular waveguide acts as an inductive element whose inductance is inversely proportional to its diameter and the waveguide dimensions [26]. The geometry and the equivalent circuit model of a shorting pin are shown in Fig. 1*b*. For this case the transformer turn ratio can be calculated from [27]

$$n = \sqrt{\frac{2a}{b}\left(\frac{\tan ka}{ka}\right)^2} \quad (1)$$

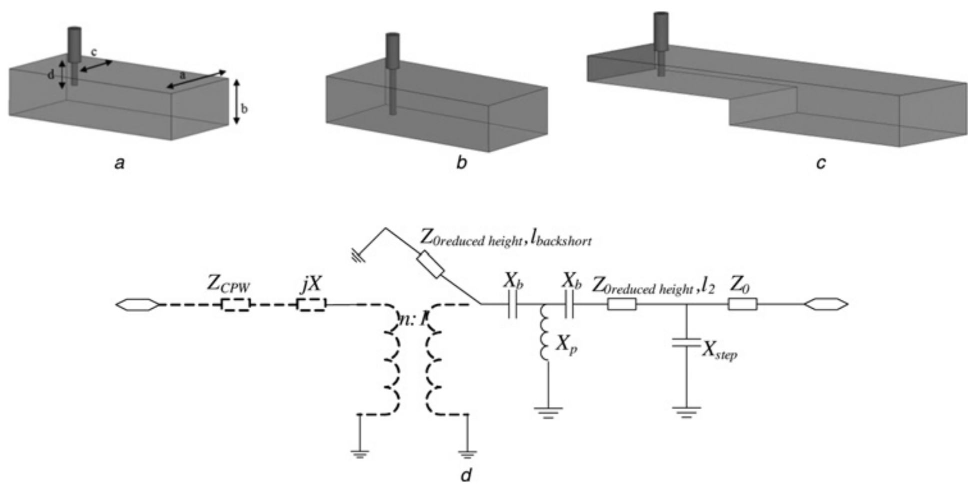

Fig. 1 *Design considerations of waveguide transitions*

a Traditional resonant probe excitation for waveguide
b Probe is terminated by the broad wall of the waveguide. In the equivalent circuit mode, L_p is the equivalent inductance (X_p), C_b is the series capacitance of the short-circuited probe (X_b) [26] and Z_0 is the characteristic impedance of the waveguide
c *E*-plane step discontinuity generates capacitances required for resonance needed for the mode conversion *c* the equivalent circuit model for the proposed resonance
d The equivalent circuit model for the proposed resonance, X_{step} is the equivalent capacitance of the step discontinuity

IET Microw. Antennas Propag., 2012, Vol. 6, Iss. 4, pp. 443–449
doi: 10.1049/iet-map.2011.0194

where a and b are the width and height of the rectangular waveguide, respectively, and k is the free space wavenumber as described in [27]. The reactance X can be estimated by variational methods [27] and is capacitive below and inductive above the resonant frequency. To compensate for the inductance of the shorting pin X_p, a capacitive element is needed. Since a step discontinuity in the E-plane of the waveguide acts as a capacitive element, it can be used to compensate for the inductive behaviour of the pin. That is, a resonant condition can be realised by terminating a short-circuited pin in a reduced-height waveguide with a step transition from the reduced-height waveguide to the standard-size waveguide as shown in Figs. 1*c* and *d*. The length of the waveguide between the pin and the step transition can be used to control the capacitance seen by the inductance. Also, the waveguide height can be used to control the capacitance at the step transition point. This structure eliminates the use of suspended probe for transition and is simple to fabricate.

3 CBCPW to rectangular waveguide transition

CBCPW lines are preferred at very high frequencies for mounting active components because of their low-loss characteristics [28] (Fig. 2). Hence, a transition from a low-loss membrane-supported CBCPW to rectangular waveguide is considered here. In this CBCPW, since the dielectric substrate is removed and the line is suspended over a hollow trench, dielectric loss has been eliminated. Also, the conductor loss is decreased substantially by reducing the current density near the edges and distributing it more uniformly over the metallic strip and the ground around it. For fabrication purposes, a dielectric membrane on top of the line supports the suspended line over the trench. This line can be easily incorporated with hollow rectangular waveguides [28].

To design the transition based on the idea of the short-circuited pin, first the dimensions of waveguide and CBCPW line are chosen based on the desired frequency range. The initial values of elements of the circuit model are selected using the analytical formulas and measurement results reported in [26, 27]. These values along with the length of waveguide and CPW line sections are optimised using transmission line analysis of the circuit model to obtain the resonant behaviour. A structure based on these values is designed and then optimised using full-wave simulator Ansoft HFSS.

The proposed transition from CBCPW to rectangular waveguide is presented in Figs. 3*a* and *b*. In this transition, three conversion steps are required: from CBCPW to conventional CPW inside the waveguide, CPW to reduced-height waveguide and reduced-height waveguide to standard waveguide. The CPW line is narrowed as it enters the reduced-height waveguide in order to create a transmission line resonator that includes the pin. A second resonator is created between the pin and the step discontinuity inside the waveguide. The centre conductor of the CPW line is open circuited at the location of the pin and the pin is connected to the lower wall of a reduced-height waveguide. On the other side of the pin, the reduced-height waveguide is short circuited at a distance to appear as another reactance parallel to the pin inductance as shown in the equivalent circuit model in Fig. 3*c*. The discontinuity from CBCPW line to CPW line inside the waveguide is also modelled by a shunt capacitance.

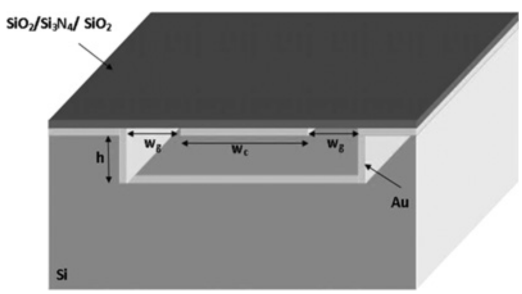

Fig. 2 *Low-loss membrane supported cavity-backed CPW [28]*

In this line, the dielectric substrate is eliminated and the centre conductor is supported by a membrane on top. The transition of this line to rectangular waveguide is investigated

To demonstrate the performance of the proposed transition a Ka-band prototype is considered. The equivalent circuit model parameters are extracted as outlined before and the S-parameters of a back-to-back structure from CBCPW to rectangular waveguide and rectangular waveguide to CBCPW based on the circuit model are shown in Fig. 3*d*. This design offers almost 9% of the bandwidth and less than 1 dB insertion loss. At the next step, Ansoft HFSS is used to analyse and optimise these values by adjusting the lengths of transition line segments, the step height and the pin thickness. The reflection coefficient of the optimised structure is compared to that of the circuit model for the back-to-back transition in Fig. 4. As shown, a good agreement is obtained. It is also shown that the physical structure provides a better performance than the one predicted by the circuit model. The electric field distribution of the optimised structure is shown in Fig. 5*a* and well represents the conversion of the CPW mode to the waveguide mode using the terminated pin. Fig. 5*b* represents the reflection and transmission coefficients of this transition. It is observed that a transmission above −1 dB and reflection below −10 dB for more than 9% of the bandwidth can be achieved. An enlarged plot of the transmission coefficient over the passband is also presented in Fig. 5*c*.

3.1 Bandwidth enhancement

The bandwidth of the transition is sufficient for most application at these very high frequencies. However, in situations where more bandwidth is needed, the number of shorting pins and step discontinuities can be increased accordingly.

To add one more resonance, another shorting pin and step discontinuity can be introduced. The geometry of a three-pole structure is shown in Fig. 6*a*. Since the height of the step discontinuity is smaller which introduces smaller capacitance values, the pin must be thinner to provide a resonance value close to the previous ones. The dimensions are optimised using Ansoft HFSS and the reflection coefficients of the structure are presented in Fig. 6*b*. It is shown that the additional resonance increases the bandwidth up to about 15%.

4 Fabrication and measurement

As mentioned before, a dielectric membrane is used to support the top suspended thin metal layer of CBCPW and prevent it from collapsing. The membrane covers the conductor and the structure cannot be fed by probes from

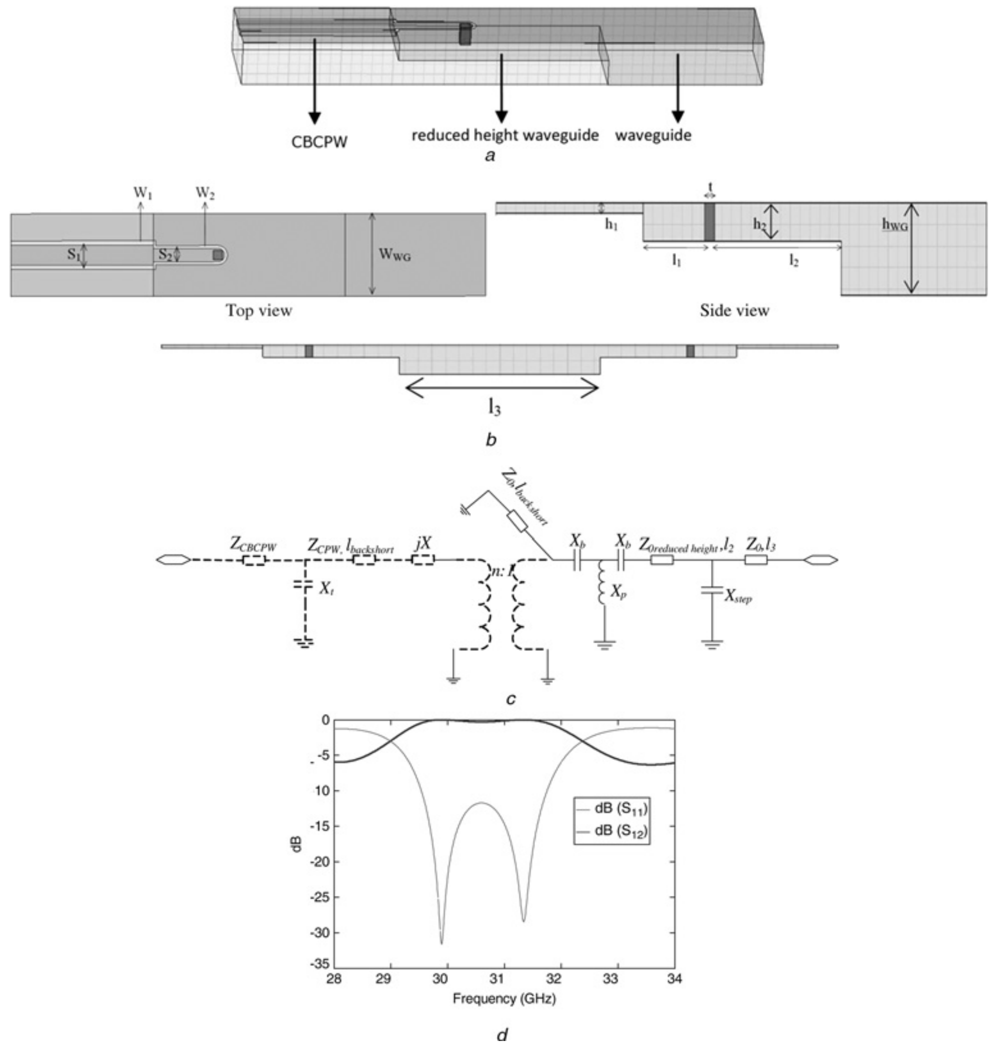

Fig. 3 *Proposed transition from CBCPW to rectangular waveguide*

a CBCPW to rectangular waveguide transition. It includes a transition from CBCPW to CPW, CPW to reduced-height waveguide mode and reduced-height waveguide mode to standard waveguide mode
b Top view, side view and a side view of the back-to-back structure
c Equivalent circuit model for the transition for $Z_{\mathrm{CBCPW}} = 50\,\Omega$, $Z_{\mathrm{CPW}} = 85\,\Omega$, $X_t = -j\ 140\,\Omega$, $X = -j\ 110\,\Omega$, $n = 1$, $X_b = -j\ 8\,\Omega$, $X_p = +j\ 58\,\Omega$, $X_{\mathrm{step}} = -j\ 1000\,\Omega$, $l_{\mathrm{backshort}} = 5\ \mathrm{mm} = \lambda_g\ /3$, $l_2 = 10\ \mathrm{mm} = 2\lambda_g\ /3$, $l_3 = 17\ \mathrm{mm}$. Waveguide dimensions are set as the standard dimensions of WR-28 Ka-band waveguides
d Reflection and transmission coefficients of the circuit model of the back-to-back structure for the initial values of the elements to achieve a low conversion loss

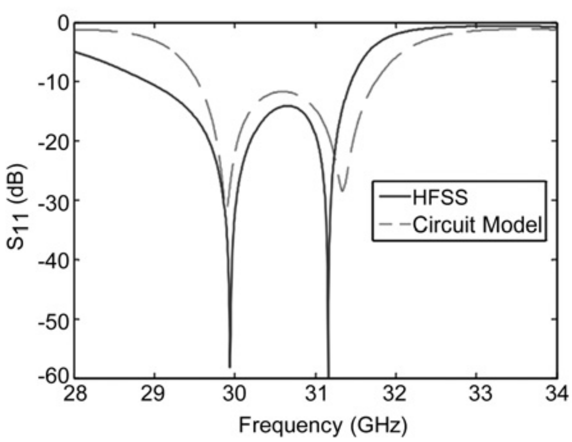

Fig. 4 *Optimised transition with HFSS is compared to the initial design based on the circuit model for a back-to-back transition and shows good agreement and improved performance*

the top. Basically the top layer and the membrane are protecting the active components that excite or receive the waveguide signal. In order to test the transition and be able to make contact to the probe, the top layer of the membrane is also patterned with a CPW line and is connected to the bottom layer through via holes as shown in Fig. 7. With this transition, the structure can be fed from the top by 50 Ω GSG probes.

To fabricate this structure at Ka-band, the lower parts including the CBCPW, reduced-height waveguide and standard-height waveguide are machined on an ultra-machinable alloy 360 brass plate and are gold-plated to prevent oxidation. Rogers Duroid 5880 with 1/4 oz (8 μm) electrodeposited copper foil is used as the top cover of the waveguide as well as the membrane for CBCPW. The thickness of the substrate is chosen to be 0.127 mm (5 mil), thin enough to act as the membrane. Both sides of the substrate are patterned and connected by metalised via holes as shown in Fig. 7. Additional vias are drilled in the substrate in order to suppress the substrate mode. The fabricated parts are represented in Fig. 8.

doi: 10.1049/iet-map.2011.0194

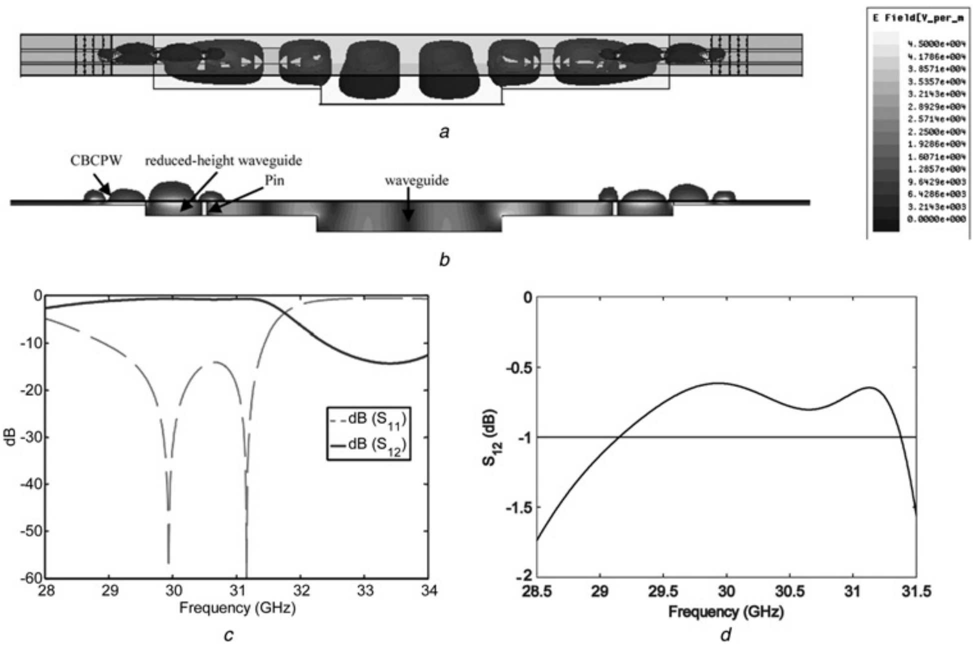

Fig. 5 *The optimised structure*

a Electric field distribution at 30 GHz for a back-to-back transition with $S_1 = 1.46$ mm, $W_1 = 0.37$ mm, $S_2 = 0.972$ mm, $W_2 = 0.247$ mm, $W_{\mathrm{WG}} = 7.112$ mm, $h_{\mathrm{WG}} = 3.556$ mm, $h_1 = 0.379$ mm, $h_2 = 1.65$ mm, $t = 0.49$ mm, $l_1 = 5.024$ mm, $l_2 = 9.97$ mm and $l_3 = 16.8$ mm
b Side view: *E*-plane cross section (waveguide centre at maximum *E*-field)
c Reflection and transmission coefficients for the back-to-back transition at Ka-band
d Transmission coefficient at the passband

Different techniques were tested to bond the substrate to the brass unit. Initially solder paste and silver epoxy were used. However, since a high temperature is needed for pastes and epoxies, the substrate was warped and damaged, and the brass unit was oxidised. Also, the results were not satisfactory because of misalignments and air gaps around the edges. In addition, the solder reflow caused short circuits in the substrate during the bonding process. Moreover, many times the thin pins were bent and easily broken during bonding at high temperatures. The best results were obtained by screwing the two units together. Since the substrate is very thin, a thick metal plate is used on top of it to ensure that sufficient pressure is applied to the substrate and brass unit to prevent possible air gaps. The silver-plated long rigid steel wires are snapped into holes drilled on the bottom of the reduced-height waveguide and soldered. The pins pass through holes cut on the substrate to facilitate alignment of the substrate and the unit.

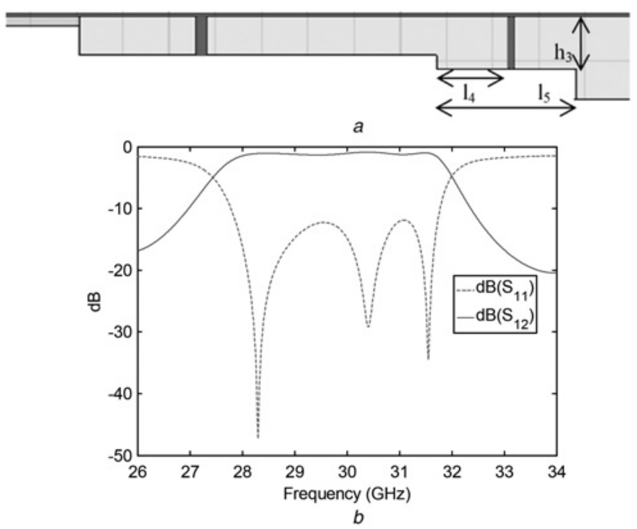

Fig. 6 *Bandwidth enhancement*

a Proposed three-pole structure for enhanced bandwidth
b *S*-parameters of the transition
Bandwidth of the transition is increased to about 15% as a result of having a three-pole structure by adding one resonance, a shorting pin and a step discontinuity with $h_3 = 2.26$ mm, $l_1 = 5$ mm, $l_2 = 10$ mm, $l_4 = 3.3$ mm, $l_5 = 6$ mm. Additional resonances can be introduced for further enhancement.

After bonding, the structure is fed by ground-signal-ground (GSG) probes connected to the network analyser using Ka-band flexible cables. Prior to measurement it is essential that the probes and cables be calibrated. For this purpose, on-substrate thru-reflect-line (TRL) calibration lines are simulated and designed. For TRL calibration, three calibration standards are fabricated on the same substrate. These include two line segments with known phase shifts for thru measurements and an open-ended line with a known electrical length for reflection measurement. After calibration, *S*-parameters of the transition are measured and presented in Fig. 9. The measurement results show a good agreement with the simulation, around 9% of the bandwidth below −10 dB for return loss and over −1 dB for insertion loss. The observed deviations from the simulation are attributed to misalignment, especially near the pin positions and possible air gaps between the substrate and the brass unit. The air gap should be of lesser concern since screws connecting the substrate to the brass unit should apply enough pressure to make good metal-to-metal contact. Since alignment is done with hand, small misalignment can lead to small deviations from the ideal response. To examine this hypothesis, a simulation was carried out where the top substrate was shifted to one side by a very small amount to produce about 300 μm translational displacement at the pin position. This is a typical length that might be misaligned by manually aligning. Fig. 10 shows the

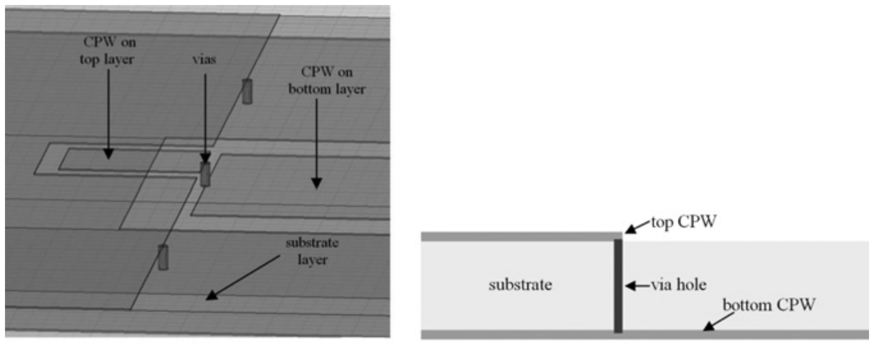

a *b*

Fig. 7 *CPW to CBCPW transition*

a Transition from a 50 Ω CPW line patterned on top of the substrate to the CBCPW line patterned on the bottom layer. Lines are connected through electroplated via holes
b Side view

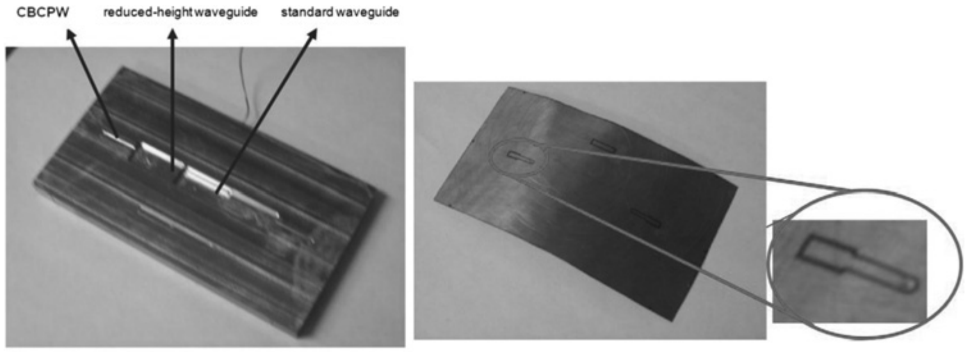

a *b*

Fig. 8 *Fabricated parts*

a CBCPW trench, reduced-height waveguide and the standard waveguide are machined on a brass plate
b Top cover includes the lines is a substrate whose both sides are etched with CPW patterns

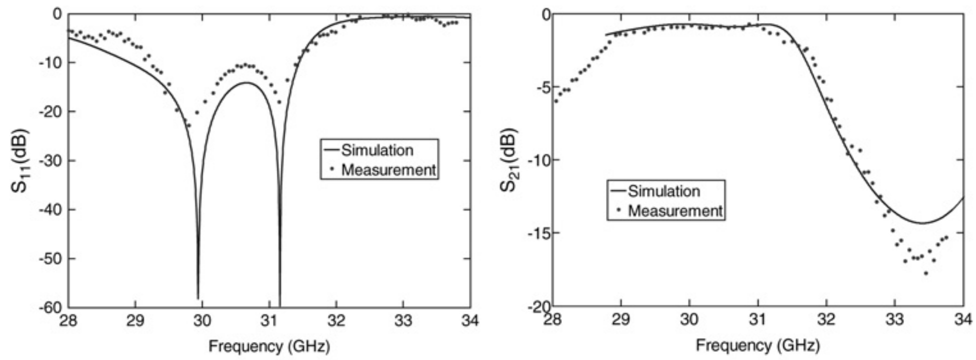

a *b*

Fig. 9 *Simulation compared to measurement results*

a Reflection coefficient
b Transmission coefficient
Both show a good agreement with the simulation. Observed deviations from the simulation are attributed to misalignment, especially near the pin positions and possible air gaps between the substrate and the brass unit

simulation results for the misaligned structure where it is shown that the transmission has decreased specifically for frequencies lower than 29 GHz. Also, the impedance match near 31 GHz is not as good as what the structure is capable of producing. This is very similar to the measured results indicating that even careful hand alignment is not good enough to achieve the best performance this transition can produce at Ka-band. To achieve better results, a better alignment approach will be needed. For the ultimate application of this transition at Y-band wafer alignment approaches in clean rooms are available for achieving alignment accuracy down to 1 μm.

doi: 10.1049/iet-map.2011.0194

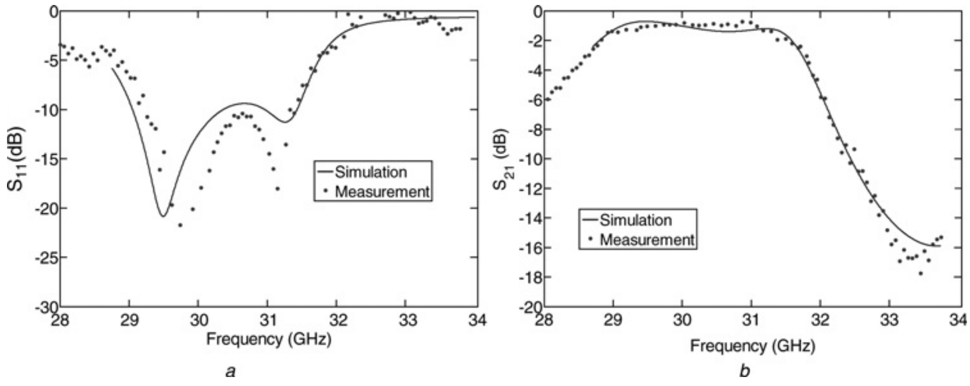

Fig. 10 *Simulation results of a structure with misalignments (300 μm translational displacement) between the top substrate and the brass unit compared to the measured results*

Transmission is decreased for frequencies lower than 29 GHz and the impedance match near 31 GHz is not as good as that of the optimised

5 Conclusion

We demonstrated a very simple and easy-to-fabricate CBCPW line to rectangular waveguide transition with prismatic features. The transition is based on the idea of resonance excitation but does not include a suspended probe which was involved in the previous transitions. Using a short-circuited pin makes the transition amenable for machining and micromachining techniques with fine tolerance needed for millimetre- and submillimetre-wave applications. An equivalent circuit model, in which lumped elements model the discontinuities and transitions, was developed for the initial design. A back-to-back structure from CBCPW to waveguide and waveguide to CBCPW was then designed, optimised and fabricated at Ka-band to validate the results. The insertion loss below 1 dB and reflection of less than −10 dB over more than 9% of bandwidth has been achieved. The bandwidth enhancement was shown by introducing an additional resonance.

6 References

1 Reig, C., Navarro, E.A., Such, V.: 'Full-wave FDTD design and analysis of wideband microstrip-to-waveguide transitions', *Microw. Opt. Technol. Lett.*, 2003, **38**, pp. 317–320

2 Grabherr, W., Huder, W.G.B., Menzel, W.: 'Microstrip to waveguide transition compatible with MM-wave integrated circuits', *IEEE Trans. Microw. Theory Tech.*, 1994, **42**, pp. 1842–1843

3 Kim, J.P., Park, W.S.: 'Network analysis of inclined microstrip-slotline transitions', *IEE Proc. Microw. Antennas Propag.*, 2000, **147**, pp. 412–416

4 Ponchak, G.E., Simons, R.: 'A new rectangular waveguide to CPW transition'. IEEE Microwave Theory Tech. Int. Microwave Symp. Digest, 1990, vol. 1, pp. 491–492

5 Dalman, C.: 'New waveguide to coplanar waveguide transition for centimetre and millimeter wave application', *Electron. Lett.*, 1990, **26**, pp. 830–831

6 Godshalk, E.M.: 'A V-band wafer probe using ridge-through waveguide', *IEEE Trans. Microw. Theory Tech.*, 1991, **39**, pp. 2218–2228

7 de Mingo, J., Moliner, A., Cameron, A.: 'Waveguide-to-coupled fin-line transition in Ka Band', *IEEE Microw. Guid. Wave Lett.*, 1996, **6**, pp. 363–365

8 Lin, T., Wu, R.: 'CPW to waveguide transition with tapered slotline probe', *IEEE Microw. Wirel. Compon. Lett.*, 2001, **11**, pp. 314–316

9 Lin, T., Wu, R.: 'A broadband microstrip-to-waveguide transition with tapered CPS probe'. Proc. 32nd European Microwave Conf., Milan, Italy, 2002, pp. 1–4

10 Hung, C., Liu, A.-S., Chien, C.-H., Wang, C.-L., Wu, R.B., *et al.*: 'Bandwidth enhancement on waveguide transition to conductor backed CPW with high dielectric constant substrate', *IEEE Microw. Wirel. Compon. Lett.*, 2005, **15**, pp. 128–180

11 Ramdane, A., Richalot, E., Picon, O., Puech, J., Lapierre, L.: 'Rectangular waveguide to CPW transition without air-bridge in the Ka-band', *Microw. Opt. Technol. Lett.*, 2007, **49**, pp. 510–513

12 Ho, T.Q., Shih, Y.: 'Spectral-domain analysis of *E*-plane waveguide to microstrip transitions', *IEEE Trans. Microw. Theory Tech.*, 1989, **37**, pp. 388–392

13 Cavanna, T., Linkowski, J.R., Suriani, A.: 'Novel W-band hermetic waveguide-to-coplanar transition'. Third ESA Workshop on Millimeter Wave Technology and Applications, Espoo, Finland, May 2003

14 Cavanna, T., Franzese, E., Limiti, E., Pelosi, G., Selleri, S., Suriani, A.: 'Coplanar-to-rectangular waveguide millimeter-wave transitions manufacturing tolerance analysis', *Int. J. RF Microw. Comput. Aided Eng.*, 2006, **16**, pp. 118–124

15 Kaneda, N., Qian, Y., Itoh, T.: 'A broadband CPW-to-waveguide transition using quasi-Yagi antenna'. IEEE Microwave Theory Technology Int. Microwave Symp. Digest, Boston, MA, 2000, vol. 2, pp. 617–620

16 Simons, R.N., Taub, S.R.: 'New coplanar waveguide to rectangular waveguide end launcher', *Electron. Lett.*, 1992, **28**, (12), pp. 1138–1139

17 Digby, J.W., McIntosh, C.E., Parkhurst, G.M., *et al.*: 'Fabrication and characterization of micromachined rectangular waveguide components for use at millimeter-wave and terahertz frequencies', *IEEE Trans. Microw. Theory Tech.*, 2000, **48**, pp. 1293–1302

18 Collins, C.E., Miles, R.E., Digby, J.W., *et al.*: 'A new micro-machined millimeter-wave and terahertz snaptogether rectangular waveguide technology', *IEEE Microw. Guid. Wave Lett.*, 1999, **9**, pp. 63–65

19 Hesler, J.L., Jui, K., Dahlstrom, R.K., *et al.*: 'Analysis of an octagonal micromachined horn antenna for submillimeter-wave applications', *IEEE Trans. Antennas Propag.*, 2001, **49**, pp. 997–1001

20 Hui, K., Hesler, J.L., Kurtz, D.S., Bishop, W.L., Crowe, T.W.: 'A micromachined 585 GHz schottky mixer', *IEEE Microw. Guid. Wave Lett.*, 2000, **10**, pp. 374–376

21 McGrath, W.R., Walker, C., Yap, M., Tai, Y.-C.: 'Silion micromachined waveguides for millimeter-wave and submillimeter-wave frequencies', *IEEE Microw. Guid. Wave Lett.*, 1993, **3**, pp. 61–63

22 Becker, J.P., Lee, Y., East, J.R., Katehi, L.P.B.: 'A finite ground coplanar line-to-silicon micromachined waveguide transition', *IEEE Trans. Microw. Theory Tech.*, 2001, **49**, p. 2001

23 Lee, Y., Becker, J.P., East, J., Katehi, L.P.B.: 'Fully micromachined finite-ground coplanar line-to-waveguide transitions for w-band applications', *IEEE Trans. Microw. Theory Tech.*, 2004, **52**, pp. 1001–1007

24 Li, Y., Pan, B., Tentzeris, M.M., Papapolymerou, J.: 'A fully micromachined W-band coplanar waveguide to rectangular waveguide transition'. Proc. 2007 IEEE-IMS Symp., Honolulu, Hi, June 2007

25 Li, Y., Pan, B., Lugo, C., Tentzeris, M.M., Papapolymerou, J.: 'Design and characterization of a W-band micromachined cavity filter including a novel integrated transition from CPW feeding lines', *IEEE Trans. Microw. Theory Tech.*, 2007, **55**, pp. 2902–2910

26 Marcuvitz, N.: 'Waveguide handbook' (McGraw-Hill, New York, 1951), pp. 271–273

27 Harrington, R.F.: 'Time-harmonic electromagnetic fields' (McGraw-Hill, New York, 1961), pp. 177–179. 425–428

28 Moallem, M., East, J., Sarabandi, K.: 'Optimally designed membrane-supported grounded CPW structure for submillimeter-wave applications'. Int. Symp. Antennas Propagation, Charleston, NC, 2009

doi: 10.1049/iet-map.2011.0194